

ELEVENTH EUROPEAN ROTORCRAFT FORUM

Paper No. 35

"THE UTILIZATION OF HELICOPTER ROTOR TECHNOLOGY  
IN THE PREVENTION OF FROST IN ORANGE GROVES"

H. Velkoff  
Department of Mechanical Engineering  
The Ohio State University  
Columbus, Ohio 43210 U.S.A.

A. Sheppard  
Heli Air, Inc.  
204 Cornwall Drive  
Pittsburgh, Pennsylvania 15238 U.S.A.

September 10-13, 1985

London, England

THE CITY UNIVERSITY, LONDON, EC1V OHB, ENGLAND.

TITLE: "The Utilization of Helicopter Rotor Technology  
in the Prevention of Frost in Orange Groves"

AUTHORS: H. Velkoff  
Department of Mechanical Engineering  
The Ohio State University  
Columbus, Ohio 43210

A. Sheppard  
Heli Air, Inc.  
Pittsburgh, Pennsylvania

#### ABSTRACT

It is well recognized that during periods when orange groves are damaged by frost often a significant temperature inversion exists in the air above the grove. It was hypothesized that if the warmer air above the trees could be brought down into the grove that some of the frost damage could be mitigated. To accomplish this, a helicopter type rotor could be placed above the trees and be used to draw down this warmer air and to spread it out into the grove. The basic concept involves proper trimming of the tree skirts and a suitable match of the rotor to the grove. Analytical models of the rotor wake as it moves through the grove were developed. A series of model rotor and grove tests were conducted to provide input data to the models. A full-scale rotor was designed and tested in an orange grove. Extensive data were taken which indicated that not only could a rotor be effective in distributing air in a grove but that the flow could be modelled successfully.

#### INTRODUCTION

The recognition of the existence of temperature inversions in the air above the trees in orange groves or above the plants in a vineyard has led in the past to the use of propellers to provide mixing of the air mass and thus reduce the possibility of frost damage. The use of stationary helicopter rotors appears to offer similar benefits.

When certain atmospheric conditions exist it is possible for severe frost damage to occur to crops even though the average temperature of the air mass above the crops is considerably above freezing temperatures (1). Two factors may come into play. The first is direct radiation of thermal energy from the plants sufficient to drop the plant temperature below freezing although the air near the plant may be above freezing temperatures. The second is the direct radiation from both the plant surfaces and ground sufficient to cause the contacting air to drop below freezing temperatures while the temperatures of the air mass a few meters above the plants may be above freezing temperatures. It is also always possible for a hard freeze to occur wherein the entire air mass temperature drops below freezing due to the passage of a cold front, for example.

In the first two freezing situations, however, the temperatures of air above the trees in a grove may be significantly higher than the leaf temperatures. The use of horizontal axis propellers is a common method employed to achieving mixing of the warmer air above the grove with the colder air near the trees. The air motion achieved also enhances the heat transfer coefficient of the leaves and thus reduces the chance that radiation from the leaves to the sky can lead to frost damage.

It has been proposed that helicopter rotors be mounted above the orange groves and be used to draw in the warm air above the trees, spread the air out

through the trees, and to increase the heat transfer coefficients. The germ of the concept arose from a recognition that during a severe frost with Florida groves, it was found that using a hovering helicopter to pull the warmer air from higher elevations down into the trees led to significantly reduced frost damage.

The work presented in this paper will report on the work done to determine the characteristics of the flow field as it passes through the orange grove.

#### APPROACH

The approach considered is to mount a helicopter rotor on a pedestal positioned at a height somewhat above the trees. One or more trees would be removed at selected locations and the pedestals placed at the centers of the clearings. In operation the rotor would draw in the warmer air from above and the rotor wake would move towards the ground and upon impingement the wake would then spread radially outward. Since it was recognized that the trees would act as a "wind break" and dissipate the wake energy quickly, it is necessary to induce the air to flow along the ground and under the trees. If that could be done, then the warm air would tend to "percolate" up through the trees as it moved outwards and thus act to provide warmer air and higher heat transfer coefficients. To accomplish the ground hugging radial flow two actions are involved. The first is the natural tendency of any wall jet to remain in contact with the surface over which it flows. The second was the design concept that involves the trimming of the lower branches at the base of the trees so that a relatively free channel exists for the rotor wake to flow through. The arrangement is shown in Figure 1.

#### ANALYTICAL STUDY

An analysis was conducted which utilized a conservation of momentum approach. Prior work has been done on the spreading of both helicopter rotor wakes over the ground and the spreading of round jets which impinged on a flat surface (2,3,4). With no upper surface to dissipate the flow, such as found in these two cases, the velocity decay can be found to be of the form of

$$u/u_0 = cr^{-2}$$

A derivation of this form of equation may be found in Appendix A.

However, in the orange grove flow case, there is a very intricate upper boundary. This boundary consists of open spaces between trees, the leaves and branches of the bottom of the trees at the periphery, and the relatively empty region under the trees at the center of the trees. This flow was also analyzed on a momentum basis except that as the momentum thickness grew to a height equal to the base height of the trees, the momentum of the flow above that height was essentially lost to the flow. The radial velocity field for the case takes the form

$$u/u_0 = e^{-c_1 fx}$$

where  $x = r/r_1$ ,  $f =$  friction coefficient. The derivation of this equation may be found in Appendix A. The constants in each of the equations are related to the shear stresses/viscous actions which the flow streams experience. As is usual in fluid mechanics, equivalent skin friction coefficients or friction factors were used to determine the constants.

The equivalent skin friction coefficients used were based on a series of analyses and model tests. The analytical approach considered the friction factors,  $f$ , arising in a general shear stress form

$$\tau = \rho \frac{fV}{2}^2$$

where  $\tau$  is the shear stress  
 $\rho$  is air density  
and  $V$  is the stream velocity.

To select the values of  $f$ , considerations were given to data from wall jet tests of Chuang, as well as general skin friction data from Schlichting (5,6). Because of the complex flow along the ground, under the tree canopies, and around the tree trunks, study was made of  $f$  data obtained with pinned fin heat exchanger data. Considering a PF-9F surface, resemblance to the under-the-tree flow can be seen in Figure 2. For similar  $L/D_L$  ratios, a value of  $f = .08$  seemed representative (7).

Another approach taken was to model the upper flow effects as well as the "channel" type flow. As the flow moves through the trees it tends to flow under the trees and also up into the base of the trees. Because of this, in addition to surface viscous effects, there is a tendency for flow acceleration and deceleration to take place. This can be seen in Figure 3. Because of the large array of trees, a calculation of the equivalent  $f$  was based upon equivalent nozzle-expansion flows. The recognition that 10% of the total area was subject to such action led to an estimate of  $f = .107$ .

Based upon the study of skin friction data, heat exchanger comparison, and the nozzle-accel estimate, it was believed that the bounds on  $f$  would be  $0.04 < f < .15$ . Since the practicality of the concept was so crucially dependent on the estimate it was necessary to search out rotor ground flow data on which to base  $f$ .

#### DATA ON SPREADING ROTOR FLOW

Review of available literature on the spreading of the wakes of rotors radially indicated the work of Fradenburg, of Kuhn and of Cox and Abbott (2,3,4). Fradenburg's work used a helicopter rotor but had data for  $r/R$  ratios only out to 3.5, where  $r$  is the distance along the ground and  $R$  is the rotor radius. Kuhn used both air jet nozzles and a ducted fan to achieve the radial outflow. His data achieved  $r/R$  ratios of 6.0. Cox and Abbott tested the outflows from high velocity jets simulating jet impingement outflow. They achieved  $r/R$  ratios of over 100.

Evaluation of the data presented, revealed some differences between the data taken with pure round jets and the data obtained with helicopter flows. Because of the critical importance of the value of  $f$  and the need to provide data on which to verify and thus select a flow model, it was decided to conduct model rotor tests of the radial flow along the ground.

#### MODEL EXPERIMENTS

To achieve a higher confidence in the value of  $f$ , several model tests were conducted of rotors in hover and the ground flows measured. Two rotors were used in the tests. One had a 30 inch diameter with a 2.25 inch chord and the second a 60 inch diameter with a 2.5 inch chord. Both were untwisted and utilized NACA 0015 airfoils. Since performance of the model rotors was not of concern in these tests but rather the decay of the flow field, the precise aerodynamic characteristics of the rotors were not considered to be primary

variables in these tests. The rotors were mounted at two positions above the ground plane, at 36 inches and 43 inches. Initial tests were conducted outdoors with the model hover stand mounted upon a blacktop parking area between two buildings. The distances to the walls were similar to the dividing planes between two adjacent rotors when the rotors would be mounted in an orange grove. The spacing between the walls was 62 feet. This provided for a maximum r/R of 12.4. The arrangement is shown in Figure 4. There the location of the rotor stand relative to the ground and one wall can be seen. Flow velocity data were taken using a portable Datametric hot wire anemometer placed in a screw type traverse to provide precise vertical position of the probe. Only a single component of velocity was measured, that being the primary radial outflow velocity parallel to the ground. The hot wire anemometer was calibrated in a DISA type hot wire nozzle fixture that has been used to calibrate hot wires for both helicopter rotor flow and boundary layer measurements. To acquire data, the rotor was run up to desired speed and velocities were read at selected vertical positions at each of several radial locations along the ground.

To get an estimate of the effect of trees and foliage upon the velocity decay radially, a second series of tests were run with the model rotor as located in the previous tests, Figure 4. An array of 16 small shrubs, globe arborvita, were arranged on 16 inch centers as shown in Figure 5. They were chosen to get a reasonable model of the rotor size to shrub size as might be expected in an installation. The same hot wire traverse system was used to take data as had been used in the first tests. The probe was placed at selected positions horizontally out from the rotor. A typical sequence is shown in the figure. Two vertical positions were tested, one between the trees just above the wall boundary layer, and one along the vertical centerline of the trees to measure the general effect of foliage. The test procedure was the same as that of the first test.

The tests in both cases were run early in the morning in an attempt to get data under minimum wind conditions. Generally the winds were low, running from 2 to 8 mph. The test area was essentially closed on all four sides except for an entry corridor to the parking lot. Thus the winds at ground in the test area were quite low, 1 to 4 mph with the higher one only occurring occasionally.

#### Indoor Tests

Following conduct of these tests, and because of the concern over the wind conditions, repeat runs were made indoors to get a 'zero' reference wind condition. The same model rotor hover rig was placed in a large room whose dimensions were 30 ft by 36 ft with a ten foot ceiling. Both rotors were used. In the initial indoor tests, the vertical velocity profiles were measured at selected radial positions using the same hot wire system. The sidewall effects could be considered in the same manner as in the outdoor tests. The first indoor tests simulated flow over a smooth surface, as the floor in this case consisted of waxed tiles.

#### Under-Tree Flow Simulation

Because no data were found which could shed light on flow "under the trees" with gaps to let air "up and out" from under the trees, a test was set up with scale tree trunks and tree bases. The scale was chosen to use the 30 inch rotor to model a 60 ft diameter full scale rotor. To model the 'channels under the trees', flat round disks ten inches in diameter were attached to the tops of short round dowels as shown in Figure 6. The bottom of the dowels were attached to thin flat sheets of hardboard which formed the ground plane. The hardboard sheets were then arranged to form a simulated grove array. The configuration can be seen in Figures 6 and 7. In Figure 6 the flow moves from the rotor to

the ground then out past the simulated tree bases. The base height was chosen to match the model.

Figure 7 illustrates the array of simulated trees in a top view. A single quadrant was set up. To provide for symmetry, side walls were placed at each edge of the quadrant. To provide for balanced flow to the quadrant the blockage screens shown were put around the base of the rotor to produce an equivalent resistance to flow as found with the 'tree sector'. The proper blockage was determined experimentally. The vertical velocity profiles were measured using the same hot wire traverse system as previously used. Velocities were determined at selected radial stations and at the outer radial location at several azimuth positions.

Although this test was used to simulate the case where the flow would tend to move up and out of the channel formed under the trees, it would not, of course, be able to model the losses in the upper flow as that flow encountered the dense foliage of actual trees. It should also be noted that since the primary purpose of all the tests was the mapping of the flow field as it moved from entry under the trees to outer radial positions, that the exact nature of the rotor used was not of particular importance. Both rotors used provided similar results.

#### EXPERIMENTAL RESULTS

##### Outdoor Tests - Model Tests

Only the 60 inch diameter rotor was used in the tests conducted outdoors. After the rotor was brought up to desired speed, 750 rpm, velocity data were read at selected radial stations. Figure 8 presents results at a distance of 4 feet from the rotor center line. The rotor plane was located at 43 inches above the ground. It can be seen that a peak velocity exists close to the ground as would be expected with the start of a wall jet. A spread of  $\pm 2$  ft/sec. is shown to depict the maximum variability seen with the data. Figure 9 presents data at other radial locations as well. At 12 feet the peaked appearance has disappeared and the decrease of velocity with distance can be readily seen. Although not shown, the same  $\pm 2$  ft/sec variability exists. Figure 10 shows a comparison of profiles in the vertical direction for the cases of no 'trees' and with 'trees'. The data are shown at 20 feet from the center which is located behind the last row of 'trees'. Figure 11 presents data for the decay in velocity in the radial direction with and without 'trees'. The great change in slope can be readily seen which is a direct measure of the increased losses that the simulated trees cause.

##### Indoor Tests

Tests results with the 60 inch rotor at 43 inches above the floor are shown in Figure 12. No simulated trees exist in this case. The close similarity of the profile shape at the innermost position with similar outdoor data can be seen. They both exhibit the peaked wall jet characteristic. The data are much more consistent than the outdoor data and have a scatter of the order of  $\pm 1$  ft/sec. Figure 13 presents similar results for the 30 inch rotor. The details of the velocity profile curves at the first radial station are somewhat different, but otherwise the curves are similar. Figure 14 presents data for the velocity decay with radial distance for both rotors.

##### Indoor Tests with Simulated 'Channels'

Figure 7 showed the array of disks used to simulate the under-the-tree-and-up flow. Measurements were taken in approximately radial

positions 12 inches from each quadrant wall, at 4, 8, 12, and 16 feet. Figure 15 presents the results for the 30 inch rotor. In that figure, data are given for a  $z/R$  of 2.4 and represent two tests runs at each of the radial traverses. The data shown are the highest value read and at the higher values are within  $\pm 1$  ft/sec. At the low values the oscillations were lower than that figure. The data appear to be rather consistent. Data were also taken of the velocity profile at the outer edge of the disks, at the 16 foot location. These are shown in Figure 16. The resemblance to wall boundary layers is evident. The data also show the amount of variability in the velocity readings. Data were also obtained at 25 locations around the periphery at the disks at the 16 foot location at equally spaced azimuth positions. The peak velocity measured at each position varied from 3 to 4 ft/sec for the test at a rotor speed of 1670 rpm. The data had a mean of 3.5 ft/sec and a standard deviation of .74. This set of data served as a reference for the outer region of flow.

Using the data obtained, the various values of the friction coefficient,  $f$ , were substituted into the equation for outflow

$$u = c_1 u_o / r^2$$

The value  $f = .05$  provided a good fit as can be seen in Figure 15.

#### TEST OF 14.4 FT RADIUS ROTOR IN AN ORANGE GROVE

Tests were run in an orange grove selected near Haynes City, Florida during the period 10-12 August, 1983. The rotor used was a 14.4 ft radius, 2 bladed, rotor with constant chord of 22", and no blade twist. The rotor hub was mounted at 30 feet above the ground. The rotor speeds were maintained during tests at a reference speed of 165 rpm.

The primary purpose of the tests was to measure the flow field near the ground surface and under the orange trees out as far as acceptable data could be taken. Velocity measurements were taken using two hot wire hot film anemometers, a Datametric unit and a TSI industrial unit. Data runs were taken early in the morning on 11 and 12 August, 1983. The early hours were used in an attempt to get the lowest possible wind so that the data obtained would be indicative of still air, frost conditions. Such low wind conditions are necessary to show rotor flow effects in a realistic manner. Successful rotor operation and velocity data runs were accomplished. This section of the paper will present the procedures used, instrumentation, results, and interpretation.

#### Instrumentation

Two air velocity measurement instruments were utilized in the tests, a Datametric industrial unit, and a TSI industrial unit. (Datametric Air Flow Multimeter Model 800 VTP, TSI Industrial). Both units had three ranges available allowing accurate measurement of very low velocities from 100 feet/minute to speeds of over 5000 fpm. The instruments were calibrated using a standard hot wire facility available within the Department of Mechanical Engineering at The Ohio State University. The calibration facility consists of a settling chamber which receives shop air, screens in the chamber and a standard 3/4" diameter outlet nozzle. A probe holder keeps the hot wire sensing elements located in the nozzle flow at the core of the jet flow. Pressure in the chamber is monitored using an inclined manometer which is leveled and zeroed prior to data runs. The temperature of the air flow is measured either in the chamber, or out in the jet at low speeds, using a mercury-in-glass laboratory thermometer. The outlet pressure is the room pressure which is obtained from a precision laboratory mercury barometer located in the same room. The air density is calculated from the measured pressures and temperature. The

reference flow velocity is calculated using Bernoulli's incompressible equation, with the measured pressure change (manometer) density and nozzle coefficient.

Data were taken for a wide velocity range with both instruments. It should be noted that the "hot wire probe" for the TSI unit was a single round rod and is not considered to be highly directionally sensitive. The single wire probe of the Datametric unit needs merely to be placed approximately perpendicular to the flow to get good data. During the actual tests such precautions were observed. The calibration equation for the TSI probe was obtained as:

$$V = .019y \quad \begin{array}{l} V \text{ is in ft/sec} \\ y \text{ is reading in cfm} \end{array}$$

The calibration curve for the Datametric probe was obtained as

$$V = 0.0225y$$

#### Measurement Procedure

Velocity data were taken at 25 foot intervals away from the rotor center. The array of points where data were taken is shown in Figure 17. The rotor is shown as the center of the array. It was located in a space along a tree row where 2 trees had been removed. The grove extended to 150 feet east and west from the rotor. It extended to over 300 feet north and south from the rotor. Data were taken along a radius directly west from the rotor, along a 45° direction from the rotor and along a 2:1 radial line.

Velocity measurements at each of the ground locations shown, were taken at 3 inch vertical intervals from 3 inches to 48". Some difficulty was experienced in taking data at the greater distances if the probe was located within or in close proximity to the tree leaves. It should be noted that the nominal base tree height was three feet. Each test sequence would start along a selected azimuth (west for example) at the 25 foot radius point once the desired rotor speed (165 rpm) was reached. The probe would then be positioned at each vertical location and the velocity scale read.

Because of the amount of sand and particles that were thrown outward by the rotor flow, the more rugged TSI Industrial unit was used as the primary instrument. One test was run using the Datametrics Instrument as a backup. The "run-for-record" tests started just after dawn at approximately 7:30 a.m. at which time there was a background wind of about 50 ft/min from the southwest. By the time the North-North-West data were taken, the wind had increased to over 100 ft/min and affected the readings at the outer radii positions.

The tests run on the next day were started earlier, at approximately 6:30 a.m., to obtain lower wind conditions. The background wind was about 20 ft/min. It rose up to slight gusts of 200-300 ft/min at the conclusion of the last test. In general, the data for all tests had winds at or below 20-30 ft/min.

All readings that were taken displayed large fluctuations. These were due to the large scale turbulent fluctuations that exist in any rotor flow. The fluctuations are due to the intense, concentrated vortices that exist in a rotor wake. Average values of the scale readings were noted after observing the scale pointer for a period of time that would range from 10-30 seconds at each vertical position. It is believed that the data taken represent good averages and are within ±10% of the actual average velocities.



## Data Presentation and Results

The data taken were the velocities at each of the ground array points and vertical positions. The shape and pattern of the velocity field in the grove due to the rotor flow is shown by means of plots of the scale readings of velocity vs. height for various radii for each test case. Figures 18-22 depict the pattern of the velocity fields. Review of the curves and data points on each of the figures reveals that the data appears to be consistent with logical trends shown. The trends shown are considered good. Since the data are the actual calibrated velocities the scatter at  $r_g = 25$  feet is due primarily to the conditions of rotor flow at the first radius position. Differences in rotor speed, thrust, tractor location relative to the position all could affect this. The decay of average velocity with radius is similar to what was seen in model tests.

In order to compare with theory the data were non-dimensionalized and normalized to a reference at the first radial station for each case. That is, for each test run, the average of the peak velocities at each station were divided by the average velocity at 25 feet radius for that test. These data were then plotted versus radius and are shown in Figure 23.

It can be seen that much of the previous scatter is reduced. Close study of the data reveal that the 2:1 N-NW radius data show lower velocities away from the rotor center than either the 0°-West case, or the 45° NW cases.

To correlate the data with the theories, it was necessary to adapt the theories to the specific configuration used in the tests. The two theoretical equations

$$u = c_1 e^{-c_2 r} : - \text{with up flow}$$

$$u = c_3 r^{-2} : - \text{outflow only}$$

had to be modified so that the reference velocity was that at  $r = 25$  feet, and where  $r_1$  reference was feet. The equations become

$$u = u_1 e^{-\frac{f r_1}{2 h_1} (x-1)} : \text{with upflow}$$

$$u = u_1 \left(1 + \frac{f r_1}{4 h_1} (x^2 - 1)\right)^{-1} : \text{outflow only}$$

where for this case

$$r_1 = 25 \text{ feet}$$

$$h_1 = 3 \text{ feet}$$

$$x = r_g / r_1$$

$$r_g = \text{ground radial position, feet}$$

The upflow equation is plotted in Figure 23 for various values of  $f$ . It can be seen that almost all of the data fall within the band of  $0.1 < f < .12$ . The value of  $f$ ,  $f = .107$ , seems to provide a good average value. It can also be observed that a higher value of  $f$  correlates best with 2:1 direction data. A lower value of  $f$ , correlates best with the 45° and west directions.

As a check with the outflow theory, that equation and the data are plotted in Figure 24. The  $f$  value range is from  $f = 0.06$  to  $.12$ . Although the curves for the outflow theory fit well in the region of smaller radii, in the outer regions (after passage through several trees) the trends predicted are too optimistic. From study of the Figures 23 and 24, it appears that the upflow

theory does a much better job of predicting the ground flow velocities at the larger distances.

Flow quantity with radial position was also calculated based upon the "average" velocity used previously to get a "measure" of the flow. The flow quantity was determined simply as follows

$$Q = 2\pi r g_i h_i V_{av}$$

with  $h_1 = 3'$  chosen since this relates to the flow carried under the trees. The result is shown in Figure 25. Assuming that  $u_0 = 1/2 u_1$ , or that velocity of disk is 1/2 the flow in the rotor wake, then the quantity through the rotor would be 14000 cubic feet per second. It can be observed from the figure that the quantity of flow in the wake just out from the rotor is higher than that through the rotor. This is possible because of the entrainment of "outside the rotor" air into the moving wake by the large scale turbulence of the wake. Further cut, the radial quantity decreases as expected as the air moves up into the trees.

#### EVALUATION AND CONCLUSIONS

The data taken appear to be quite consistent and representative of what can be expected of a rotor of this type acting within an orange grove. With the 14.4 foot radius rotor with  $h_1 = 3$  feet it appears that measurable flow was readily found out to 200 feet radius. It also appears that the theory based upon up flow

$$u = u_1 e^{-(fr_1/2h_1)(x-1)}$$

correlates quite well with the data with  $0.1 < f < .12$ . It should be noted however, that in the 2:1 (or 20-25° azimuth) position a higher value of  $f$  is indicated, i.e.  $f = 0.15$ .

It is also apparent that the value of  $f = 0.107$  obtained from the model tests as modified by the accel-decel throttling provided a good fit to the data except for the 2:1 case. Because of the numerous assumptions used in the determination of  $f$ , such good agreement must be considered to be fortuitous.

The full scale tests verified the predictions of the analytical model that useable flows would be available at large distances from the rotor centerline if reasonable  $f$  values could be achieved. The results provide strong support for the concept of using stationary helicopter type rotors to assist in the presentation of frost damage to orange groves.

The results of studies of the heat flux and heat transfer involved in the process will be presented in a subsequent paper.

## REFERENCES

1. Bartholic, J.F. and Wiegand, C.L., "The Environment in a Citrus Grove with and Without Heater Blocks during Cold Conditions," Proceedings First International Citrus Symposium, Vol. 2, 1969 (Also Agriculture Research Service), Weslaco, Texas.
2. Cox, M. and Abbott, W.A., "Studies of Flow Fields Created by Single Vertical Jets Directed Downwards upon a Horizontal Surface," ARC C.P. No. 912, London, 1967.
3. Fradenburg, E.A., "Flow Field Measurements for a Hovering Rotor near the Ground," Fifth Annual Western Forum, Am. Heli. Soc., September 1958.
4. Kuhn, R.E., "An Investigation to Determine Conditions under which Downwash from VTOL Aircraft will Start Surface Erosion from Various Types of Terrain," NASA TND-56, Sept. 1959.
5. Chuang, T.H., "Heat and Mass Transfer to a Subfreezing Surface in a Non-Uniform Electric Field," The Ohio State Univ. Research Foundation, TR-9, Contract DA-31-124-ARO-D-246, Columbus, Ohio, Sept. 1968.
6. Schlichting, H., "Boundary Layer Theory," 6th Ed., McGraw-Hill, New York, 1968.
7. Kayes, W. and London, A.L., "Compact Heat Exchangers," 2nd Ed. McGraw-Hill, New York, 1964.

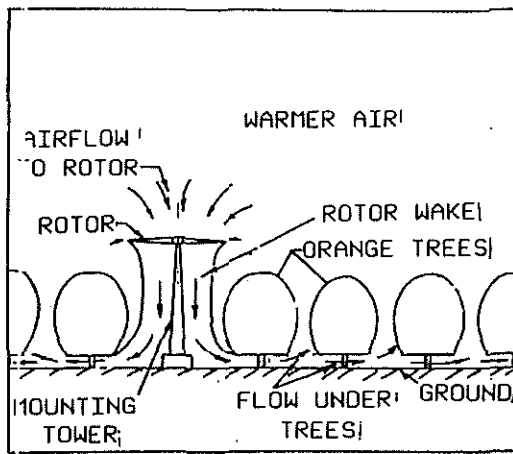


Figure 1. Flow from rotor through orange groves under trees.

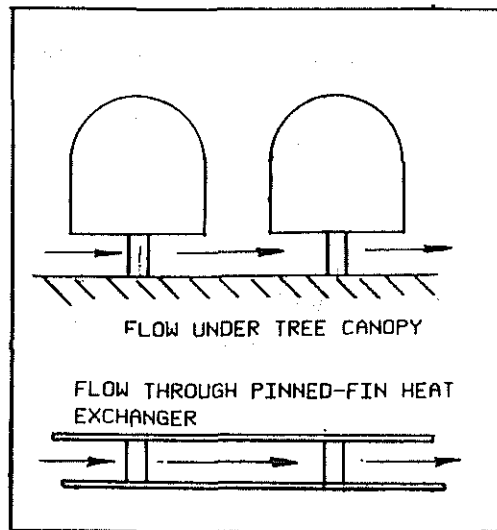


Figure 2. Comparison of flow under trees with heat exchanger flow.

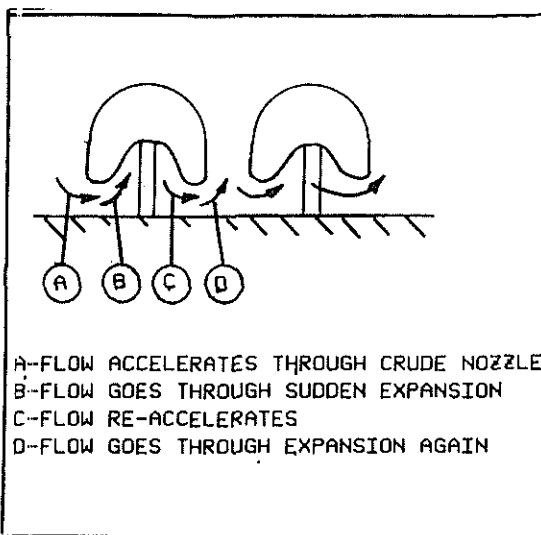


Figure 3. Acceleration-deceleration of flow under trees

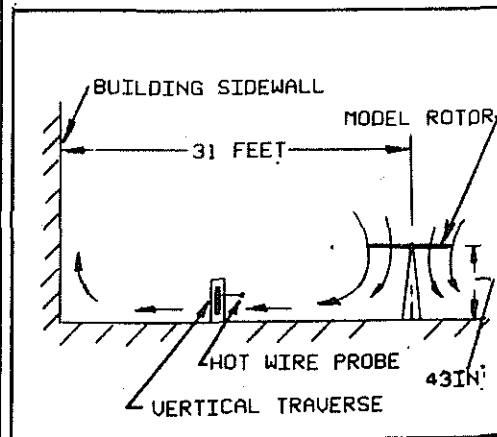


Figure 4. Model rotor test between buildings.

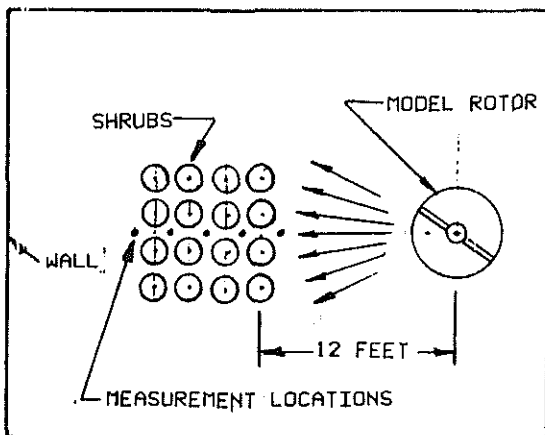


Figure 5. Model of flow through trees using shrubs.

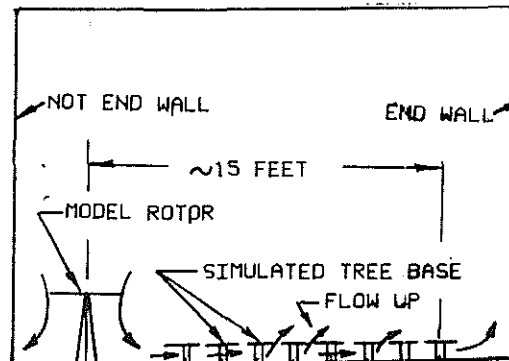


Figure 6. Flat tree model of trees

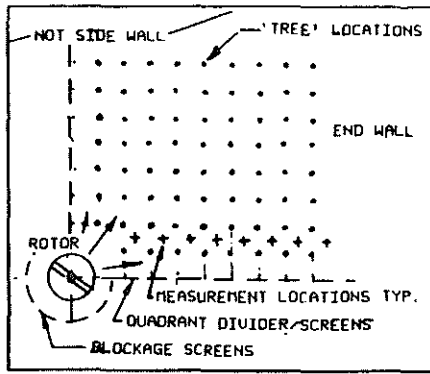


Figure 7. Arrangement of trees for below skirt flow.

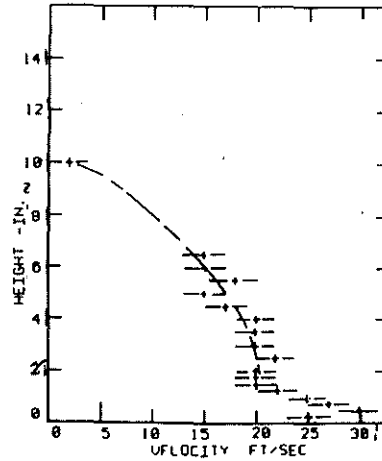


Figure 8. Outdoor Model Test velocity profile at 4 feet. 60 in. dia. rotor.  $Z = 43$  in.  $N = 750$  rpm.  $\rho = 0.0745$  #/ft<sup>3</sup>

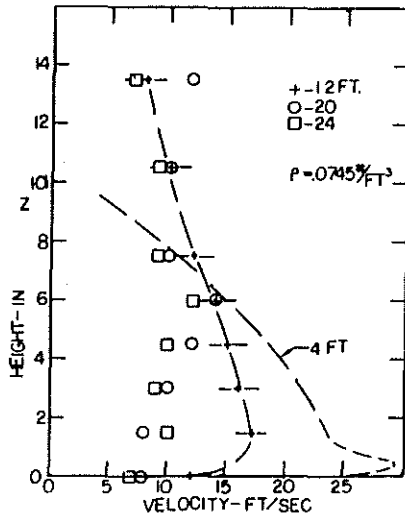


Figure 9. Outdoor Model Test velocity profiles at several radial stations. 60 in. dia. rotor.  $N = 750$  rpm.

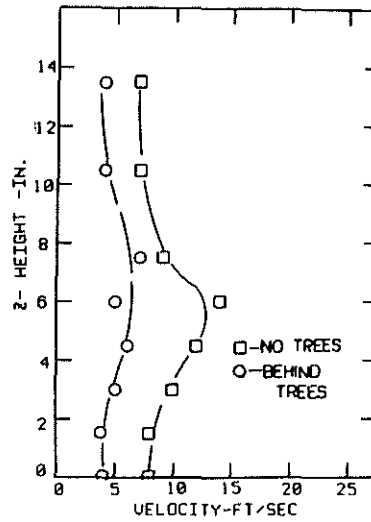


Figure 10. Outdoor Model Test comparison of 'tree'/'no tree' cases. 20 foot location. 60 in. rotor.  $\rho = 0.745$ .  $N = 750$  rpm.

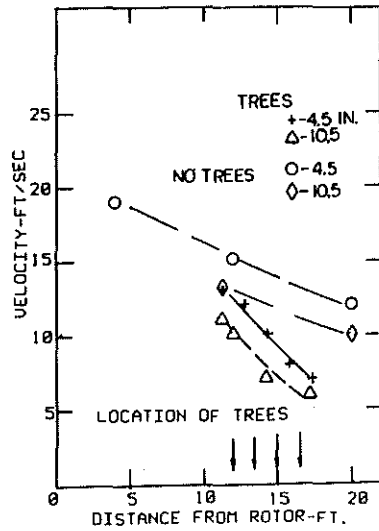


Figure 11. Outdoor Model Test Data - velocity decay of 'tree'/'no tree' cases.  $N = 750$  rpm. 60 in. rotor.  $\rho = 0.0745$ .

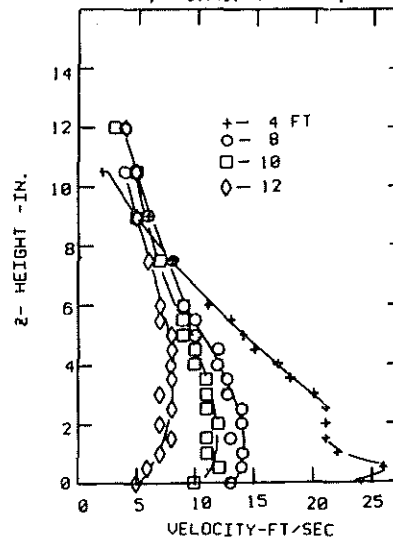


Figure 12. Indoor tests of 60 in. rotor, velocity profiles  $N = 750$  rpm,  $Z = 43$  in.  $\rho = 0.0735$ . No 'trees'.

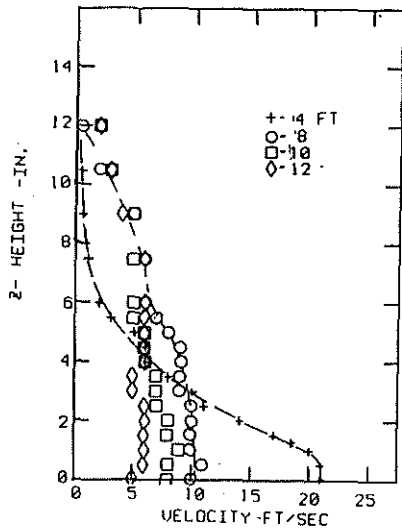


Figure 13. Indoor tests of 30 inch rotor. Velocity profiles  $Z = 36''$ .  $N = 2000$ .  $\rho = .0735$ . No 'trees'.

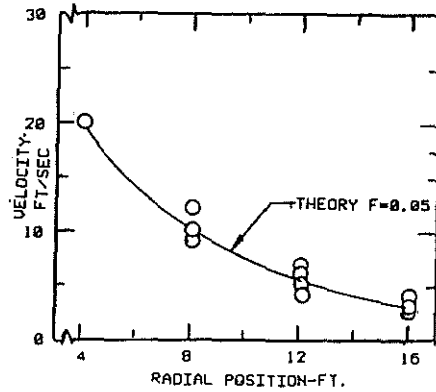


Figure 15. Velocity decay with distance with 'trees'. Mean velocity below 1.5 inches. Data from 2 locations 12" from each quadrant wall. 30 inch rotor.  $Z = 36$  in.  $\rho = .0735$ .  $N = 2000$ .

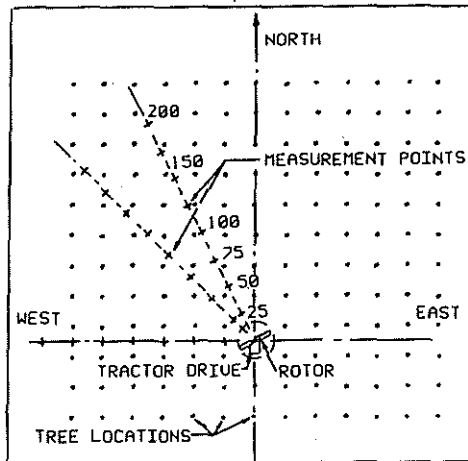


Figure 17. Arrangement of full scale rotor in orange grove.

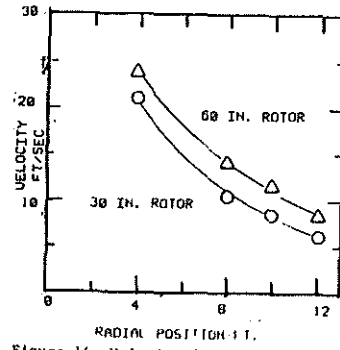


Figure 14. Velocity decay with distance. 60 inch and 30 inch rotors. Data taken 12 inches from quadrant wall. No 'trees'. Peak value of velocity.

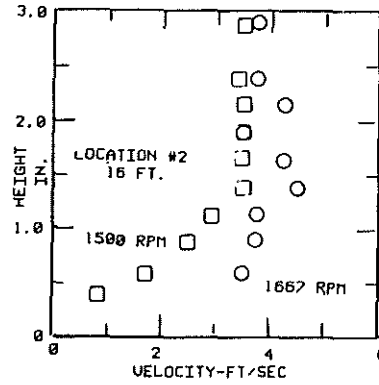


Figure 16. Typical velocity profiles for indoor 'tree' tests. 30 inch rotor. Location 16 feet from rotor center.  $N = 2000$  rpm.  $\rho = .0735$ .  $Z = 36$  in.

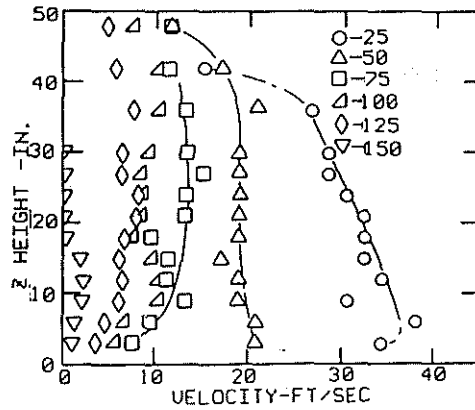


Figure 18. Velocity profiles in grove. West direction.  $N = 165$  rpm.

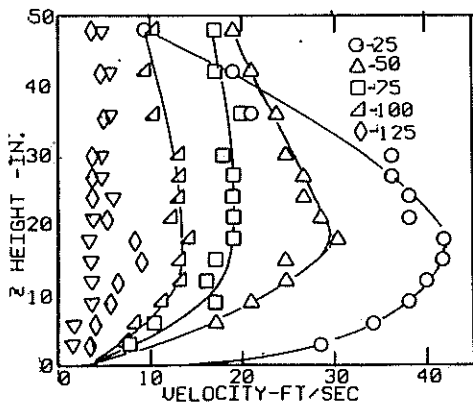


Figure 19. Velocity profiles in groove. 45°-NW direction. N = 165 rpm.

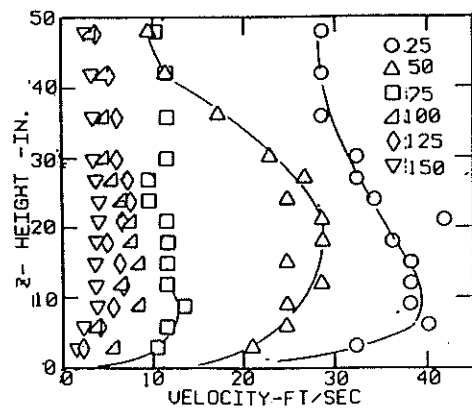


Figure 20. Velocity profiles in groove. 2:1 N-NW direction. N = 165 rpm.

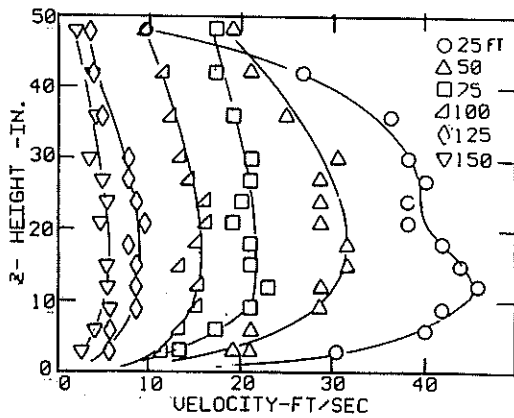


Figure 21. Velocity profiles in groove. Test #2, 45°-NW direction. N = 165 rpm.

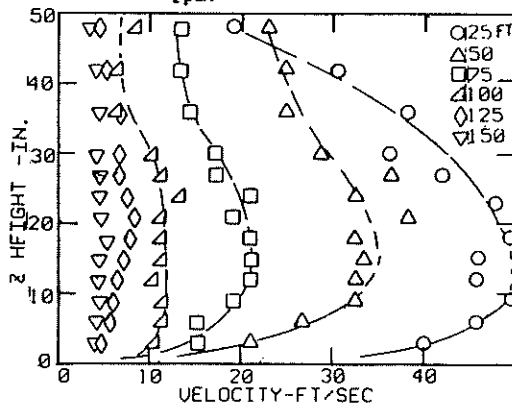


Figure 22. Velocity profiles in groove. Test #2. 2:1 N-NW direction. N = 165 rpm.

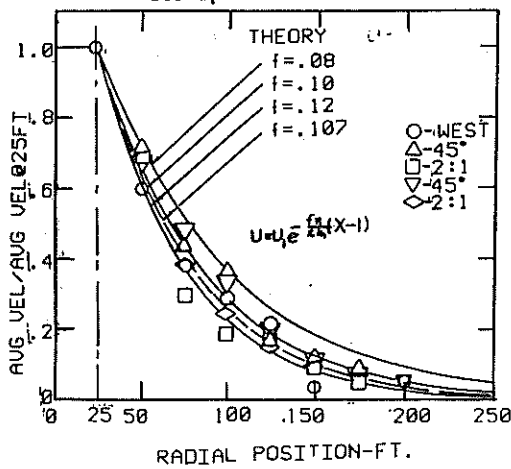


Figure 24. Normalized velocity decay with distance and comparison with outflow theory.

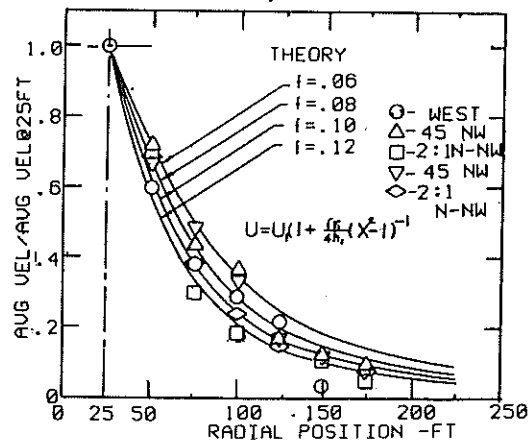


Figure 25. Variation of quantity of flow versus radial distance.

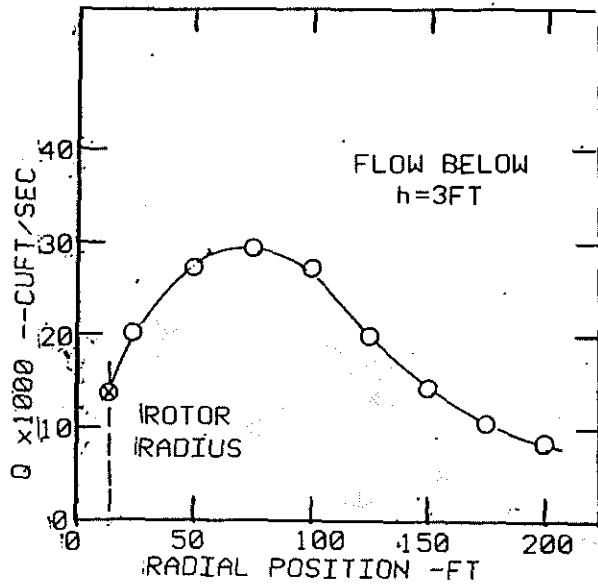


Figure 25. Variation of quantity of flow versus radial distance.

LIST OF SYMBOLS

- $D_L$  = hydraulic diameter
- $f$  = friction factor
- $h$  = height under trees
- $h_1$  = height under trees at entry to trees
- $L$  = hydraulic length
- $Q$  = flow quantity
- $r$  = radial distance
- $r_1$  = radial distance at entry to trees
- $r_g$  = radius along ground - full scale tests
- $R$  = rotor radius
- $u$  = velocity in radial direction
- $u_o$  = reference velocity in radial direction
- $x$  = ratio,  $r/r_1$
- $y$  = reading of anemometer
- $\rho$  = density in #m/cu ft
- $T$  = shear stress



APPENDIX

Analysis of Spreading Flow

Two cases were considered. The first is a simple axisymmetric flow expanding in a radial direction. It is assumed that the density is constant, and that body forces are negligible in this case. The coordinate system and the flow element can be seen in Figure A1.

Radial Outflow Only:

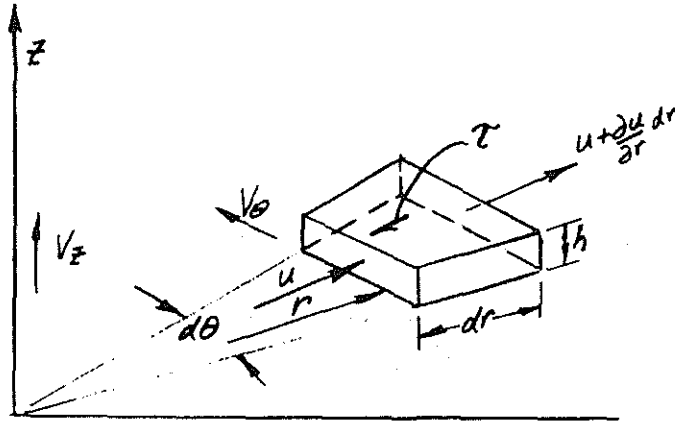


Figure A1.

It is logical to assume that  $V_\theta = 0$ ,  $V_z \ll u$  and that the pressures are everywhere equal to atmosphere.

Using a momentum balance on the fluid element and a shear stress at the surface,  $\tau$ , force per unit area,

$$\dot{m}(u + \frac{\partial u}{\partial r} dr) - \dot{m}u = -\tau r d\theta dr$$

Using the shear stress in the form

$$\tau = \rho f u^2 \frac{z}{2}$$

$$\dot{m} du = -f \frac{\rho u^2}{2} r d\theta dr$$

Assuming no entrainment, the mass flux,  $\dot{m}$ , is constant and is given by  $\rho u r h d\theta$ . At a selected radius at entry to the trees,

$$\dot{m} = \rho u_1 r_1 h_1 d\theta$$

Substituting, we obtain

$$du/u^2 = - (f/2u_1 r_1 h_1) r dr$$

Integrating

$$1/u = (f/4u_1 r_1 h_1) r^2 + c$$

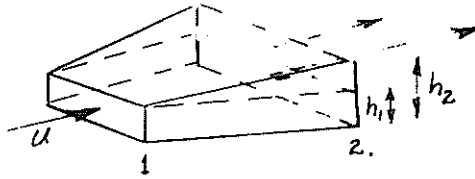
and thus we see that  $u \propto r^{-2}$

This form is analogous to the correlation equation used by Cox and Abbott (2). A more useful form can be obtained by considering the initial condition when  $u = 2u_0$  at the surface. For this case if  $u = 2u_0$  at  $r = r_1$ ,  $u = u_1$ ,  $h = h_1$ . If we equate the mean flow through the rotor,  $u_0 R^2$ , to the flow at  $V_1$ ,  $2\pi r_1 h_1 u_1$  solve for the constant of integration, and let  $x = r/r_1$

$$u = u_1 [1 + (f r_1 / 4 h_1) (x^2 - 1)]^{-1}$$

Radial Outflow with Flow Up into Trees

Consider the momentum element



Flow enters the pie shaped segment at 1. As the flow moves, its thickness grows due to the reduction in the radial velocity. Any flow moving above the tree skirt height is assumed to have been removed from the system and cannot contribute momentum. Only the fluid below  $h = h_1$  can be included in the momentum balance. Thus

$$\dot{m} = \rho u r d\theta h_1$$

The force balance becomes

$$\rho u r d\theta \cdot h_1 du = f \rho u^2 r d\theta dr/2$$

and

$$-(f/2h_1)dr = du/u$$

at  $r = r_1$ ,  $u = u_1$ ,  $h = h_1$  as before.

Let  $x = r/r_1$ ,  $\beta \triangleq f r_1 / 2 h_1$ ; then,

$$u = u_1 e^{-\beta(x-1)}$$

which is an exponential decay.

Comparison of both theories can be seen in the body of the work.